JOURNAL OF CATALYSIS **162,** 268–276 (1996)
ARTICLE NO. 0284

FTIR Studies on the Acidity of Sulfated Zirconia Prepared by Thermolysis of Zirconium Sulfate

E. Escalona Platero,[1] M. Peñarroya Mentruit, C. Otero Areán, and A. Zecchina[2]

Departamento de Química, Universidad de las Islas Baleares, 07071 Palma de Mallorca, Spain

Received October 26, 1995; revised March 18, 1996; accepted April 25, 1996

Sulfated zirconia having a BET surface area of 90 $m^2 g^{-1}$ and a temperature-resistant mesoporous texture was prepared by thermolysis (at 1000 K) of zirconium sulfate. Infrared studies of surface sulfates, CO adsorption at 77 K, and room temperature adsorption of pyridine showed close similarity to sulfated zirconias prepared by impregnation or doping from the gas phase. Four main families of Lewis acid centers were found, which gave CO adducts characterized by stretching frequencies of 2212, 2202, 2196, and 2188 cm^{-1}. Interaction of CO (at liquid nitrogen temperature) with surface hydroxyls (in partially hydroxylated samples) was found to shift the O–H stretching frequency from 3650 to 3510 cm^{-1}, due to formation of hydrogen-bonded OH···CO complexes. This downward shift, $\Delta\nu_{OH} = 140$ cm^{-1}, is significantly larger than the corresponding value for pure zirconia ($\Delta\nu_{OH} = 90$ cm^{-1}), which strongly suggests enhancement of the Brønsted acidity. Samples showing the acidic OH group at 3650 cm^{-1} were found to contain also disulfate groups and traces of molecular water. Surface hydroxyls in sulfated zirconia still appear, however, to be weaker Brønsted acid sites than are bridging OH groups in zeolites.

1. INTRODUCTION

Sulfated metal oxides with high surface area are systems of current interest in catalytic research because of their enhanced surface acidity, which confers on them a high activity in several catalytic processes, among which skeletal isomerization of alkanes is the best example. In particular, sulfated zirconia was reported to achieve isomerization of light alkanes at mild temperatures (1–7) (in the 373–573 K range), and even at room temperature in the case of sulfated ZrO_2 doped with oxides of iron and manganese (8). These processes do not take place with appreciable yield on pure zirconia. However, despite the large amount of research already devoted to the subject, the precise nature of the active sites in sulfate-doped metal oxides is not yet understood. Aprotic Lewis acid sites and protonic Brønsted acid centers both were attributed with a role in the catalytic reaction, and synergy between both centers was also postulated. Moreover, according to Kazansky (9), surface anions (Lewis basic centers) should play a key role in protonation of olefins by a neighboring Brønsted acid site, and this has strong implications for processes involving carbocations as intermediate species.

It is also known that the nature and strength of active sites in sulfated zirconia can be dependent (to some extent) on preparation conditions, such as the nature of the oxide precursor, the sulfate-doping procedure, or the activation temperature. Most researchers prepare their materials by impregnating a zirconia hydrogel with either sulfuric acid or an aqueous solution of ammonium sulfate, following with calcination at a suitable temperature. Doping from the gas phase ($SO_2 + O_2$) is also a procedure used (10). Some of us have recently shown that thermolysis of zirconium sulfate can be a convenient alternative route for the preparation of sulfated zirconia (11). Mesoporous materials prepared in this way retain a high surface area even after calcination at high temperature (12), which is not usually the case with gel-derived zirconias. The reason for this temperature-resistant porous texture is most likely to rest in the high temperature at which metal sulfates thermolyse and in the large volume of evolved gases. This leads to a consolidated mesopore system which was also observed for sulfate-derived γ-alumina (13). A further advantage of using metal sulfates as precursors of sulfated oxides is the avoidance of impregnation procedures or doping from a gas phase.

Infrared studies on sulfated zirconia prepared by the conventional (impregnation) method were reported by several authors (1, 6, 7, 10, 14–22); they include the use of pyridine (1, 3, 6, 15–17, 20, 22) and CO adsorption at room temperature (6, 7, 10, 15–18, 21, 22) as spectroscopic probes of surface acidity. However, none of these studies has included CO adsorption at low temperature. The main aims of the present work have been: (i) to examine the surface chemistry of sulfated zirconia derived from zirconium sulfate and to compare the results with corresponding data for materials prepared by the conventional route, and (ii) to test surface acidity by low temperature CO adsorption. It will be shown that this leads to information

[1] To whom correspondence should be addressed.
[2] On sabbatical leave from the University of Turin.

0021-9517/96 $18.00

on surface sites which goes beyond what can be discerned by room temperature studies alone. Preliminary results on CO adsorption at room temperature on zirconia samples similar to those used in the present work were reported elsewhere (11).

2. EXPERIMENTAL

2.1. Sample Preparation and Characterization

Details on the preparation and characterization of the parent material (sulfated zirconia) used in this work have been described (12). Briefly, $Zr(SO_4)_2 \cdot 4H_2O$ (BDH, analytical grade) was calcined at 1000 K for 5 h to achieve total thermolysis. The resulting material (subsequently called SZ) was found to have a BET surface area of 90 $m^2 g^{-1}$ and to be mesoporous. Pore size distribution was found to be unimodal, with a maximum (most frequent pore radius) at 8 nm. No contribution from microporosity was evident. Note that 90 $m^2 g^{-1}$ is a rather high value of surface area for a sample calcined at 1000 K. For comparison, zirconia powders prepared from dehydration of zirconia gels preserve a surface area of only 40–50 $m^2 g^{-1}$ after prolonged calcination at 873 K (23–25).

Chemical analysis of sample SZ showed a sulfur content of 1.1%, presumably due to tenaciously held SO_3 (self-generated during thermolysis of the starting material). Assuming that corresponding sulfate groups are all exposed at the oxide surface, this would give a statistical coverage of about 40–50% of a monolayer. Powder X-ray diffraction showed the material to be mainly in monoclinic form, with about 15% in the form of tetragonal polymorph. Samples obtained from SZ (see below) were also found to be mainly monoclinic.

2.2. Infrared Studies and Sample Nomenclature

The sample SZ was compressed into a self-supporting wafer (about 0.03 g cm^{-2}) and heated inside an IR cell similar to the one described by Marchese *et al.* (26), for cumulative periods of 30 min at increasing temperatures: 673, 873, 1073, and 1173 K. These thermal treatments (aimed at progressive reduction of sulfate content) were carried out under a dynamic vacuum: residual pressure $<10^{-4}$ Torr (1 Torr = 133.3 N m^{-2}). Samples thus obtained will hereafter be called SZ*x*, where *x* denotes the last temperature. Thus, SZ873 stands for an SZ sample heated at 673 K for 30 min followed by additional 30 min at 873 K.

At the end of each heat treatment the IR cell was transferred, whilst still under vacuum, into the IR spectrometer and dosed with appropriate amounts of CO or pyridine. Spectra were collected using an FTIR Bruker 66 spectrometer operated at 3 cm^{-1} resolution. All spectra were obtained at liquid nitrogen temperature except in the case of adsorbed pyridine, which was studied at room temperature.

3. RESULTS AND DISCUSSION

3.1. Infrared Spectra as a Function of Sulfate Content

Figure 1 shows the IR spectra in the 1450–850-cm^{-1} region of samples SZ873, SZ1073, and SZ1173. Sample SZ673 was not included because some remaining molecular water was observed, which complicated the spectrum. However, in order to follow in more detail the spectral changes upon decreasing sulfate content, three spectra were added (between SZ1073 and SZ1173) which correspond to an SZ1073 sample further heated at 1073 K for increasing time (up to 2 h). The intense band in the 1450–1340-cm^{-1} region (S=O stretching) has several components. For sample SZ873 (spectrum 1) this band shows a pronounced maximum at 1398 cm^{-1}, and a broad tail on the low-frequency side. The 1398-cm^{-1} component is also present in spectra 2 and 3, and disappears from spectrum 4 onwards. Components at lower frequency (1385–1340 cm^{-1} range) are seen to change relative intensity and to shift slightly towards lower wavenumbers with decreasing sulfate content.

In agreement with several authors (16, 17, 19), we assign the 1398 cm^{-1} band to a disulfate species of the type depicted in Scheme I (species 1), and the bands at lower frequency to the S=O stretching of a surface monosulfate (sketched as species 2 in Scheme I). Monosulfates with geminal S=O groups (species 3) have also been hypothesized (1, 27) in sulfated zirconias, but the isotope exchange experiments described by Bensitel and co-workers (19) seem to rule them out.

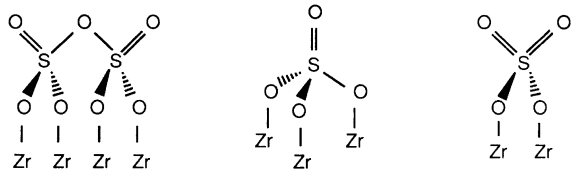

1 2 3

SCHEME I

The multiplicity of components in the 1385–1340-cm^{-1} region can easily be explained in terms of surface heterogeneity, which must yield monosulfate species with slightly different spectroscopic manifestations. In the same context, the multiplicity of bands observed in the S–O stretching region (1150–850 cm^{-1}) provides further proof for the presence of several families of surface monosulfates.

We shall not analyze these spectra in further detail, since the general features coincide with those already discussed by previous authors (19, 21). However, we wish to emphasize the following points: (i) Disulfates are only present in the most concentrated samples (as expected), and they disappear when the surface coverage decreases to less than

FIG. 1. Infrared spectra (sulfate region) of the different samples studied: **1**, SZ873; **2**, SZ1073; **6**, SZ1173; **3**, **4**, **5**, see text.

about 10% of a monolayer, on a statistical basis. (ii) Besides effects due to surface heterogeneity and the attendant desorption of different monosulfate species at different degassing temperatures, the observed shift to lower wavenumbers could have a component due to dynamic dipole–dipole interactions which are minimized at the lowest surface coverage. (iii) All of the sulfate species present in our samples are mainly (if not totally) at the oxide surface, since the 1450–1340 cm^{-1} band was observed to shift to lower wavenumbers upon adsorption of CO or pyridine (see also Section 3.3), and also minor shifts were observed in the 1150–850-cm^{-1} region. Finally, we remark that close analogy between the IR spectra in Fig. 1 and those reported for sulfated zirconia prepared by conventional methods (19, 21) provides a first proof of sample similarity.

3.2. FTIR Spectra of Adsorbed CO

Infrared spectra, in the CO stretching region, of carbon monoxide adsorbed at liquid nitrogen temperature on samples SZ673 to SZ1173 are depicted in Figs. 2 to 5. For small CO doses all samples show two IR absorption bands centered at 2212 and 2202 cm^{-1}, respectively; the high frequency one, however, is very faint for sample SZ1173 (Fig. 5). Upon increasing CO equilibrium pressure two new bands develop which are centered at 2196 and 2188 cm^{-1}. The spectra of sample SZ1173 also show additional bands at 2178 and 2168 cm^{-1}, while for samples SZ673 and SZ873 (Figs. 2 and 3) a band centered around 2165 cm^{-1} is observed in the spectra corresponding to high equilibrium pressure. This 2165-cm^{-1} band arises from interaction of CO with hydroxyl groups at the zirconia surface (see below) and will be considered at the end of this section.

Bands at 2212, 2202, 2196, and 2188 cm^{-1} are present in all of the spectra, and they saturate in succession upon increasing CO equilibrium pressure. These bands are all assigned to the C–O stretching mode of carbon monoxide interacting (through the carbon end) with Lewis acid centers of different strength: i.e., Zr^{4+} ions with varying degree of Lewis acidity. Three of these bands were also observed for CO adsorbed at *room temperature* on sulfated zirconia prepared by different methods, and this is summarized in Table 1 which also shows corresponding data for CO adsorbed at room temperature on a pure zirconia sample (ex-hydroxide). Comparison shows that the band at highest frequency is present on all sulfated zirconias, regardless of the preparation method, but not on pure zirconia. This 2212-cm^{-1} band (found at 2208 cm^{-1} in Ref. (21)) is therefore assigned to surface Zr^{4+} ions having enhanced Lewis acidity, which arises from the simultaneous presence of surface sulfate groups. Table 1 also shows that the band at 2188 cm^{-1} found in the present work was not described by previous researchers. It belongs to a species with relatively low Lewis acidity and we believe that failure to detect it before was due to not conducting low temperature experiments. Similarly, the two additional bands observed at 2178 and 2168 cm^{-1} in the spectra of SZ1173 (Fig. 5) are assigned to surface sites (Zr^{4+} ions) of low Lewis acidity. These bands were only observed after severe sulfate loss

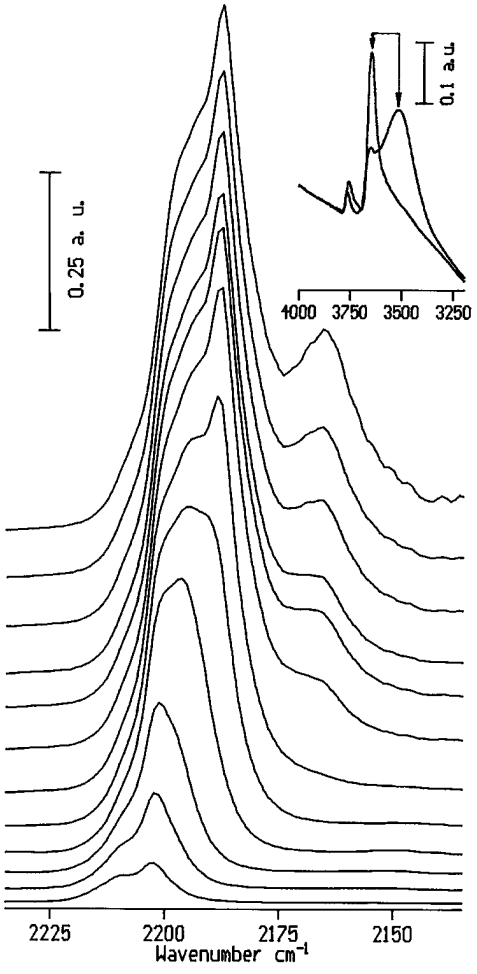

FIG. 2. Low-temperature IR spectra of CO adsorbed on sample SZ673 at increasing equilibrium pressure (from *ca.* 10^{-2} to 20 Torr). Inset shows O–H stretching region before and after dosing with CO (20 Torr).

(cf. Fig. 1), and their frequency closely corresponds to data reported by Morterra *et al.* (30) for CO adsorbed at 77 K on a highly sintered sample of pure zirconia.

It is clearly observed in Figs. 4 and 5 that bands at 2202, 2196, and 2188 cm^{-1} (measured at low CO equilibrium pressure) shift towards lower wavenumbers with increasing amounts of adsorbed CO (the behavior of the 2212 cm^{-1} band is less clear in this respect, in part because of partial overlap at increasing CO doses). This contrasts with the spectra shown in Figs. 2 and 3, where the same IR absorption bands appear at fixed wavenumbers throughout the whole range of CO equilibrium pressure. These observations can be explained in terms of adsorbate–adsorbate interactions, which can be dynamic or static (31–33). Dynamic interactions alone are known to cause an upward shift of the C–O stretching band, while static interactions usually behave in the opposite way. For CO adsorbed on metal oxides and halides, the net effect of adsorbate–adsorbate interactions is a downward shift of the C–O stretching band (33–36). This is precisely the effect observed for samples SZ1073 and SZ1173 (Figs. 4 and 5), which have a low concentration of surface sulfates. The reason why the same effect does not appear for samples SZ673 and SZ873 (Figs. 2 and 3) rests most probably in their relatively high concentration of surface sulfates, which would decouple CO oscillators.

It remains to comment on the 2165 cm^{-1} band which appears for high CO equilibrium pressure in the spectra of Figs. 2 and 3, and which (on sulfated zirconia) is reported here for the first time; we have already anticipated that it arises from OH···CO interaction. Insets in these figures show the O–H stretching region, both before and after dosing with CO. Two O–H stretching bands are observed: there is a weak one at 3750 cm^{-1} and a stronger one at 3650 cm^{-1}. They are both influenced by CO adsorption (at 77 K), but the effect is more pronounced (as expected) on the band at lower wavenumbers, which corresponds to the more abundant hydroxyl groups (and will be the only one discussed here). The fact that the 2165 cm^{-1} band is not present in

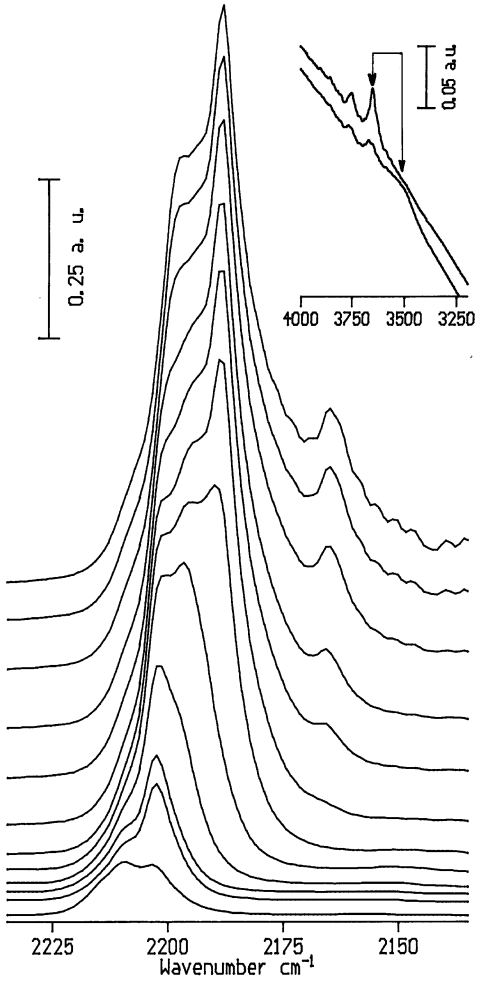

FIG. 3. As in Fig. 2, but for sample SZ873. For clarity, spectra were offset on the vertical scale, including those in the inset.

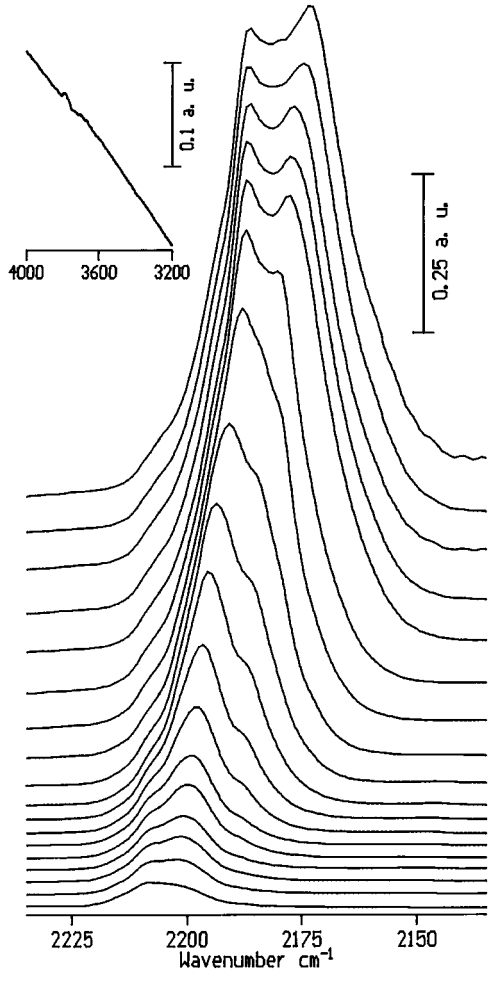

FIG. 4. Low-temperature IR spectra of CO adsorbed on SZ1073 at increasing equilibrium pressure (from *ca.* 10^{-2} to 20 Torr). Inset depicts O–H stretching region showing (practically) total dehydroxylation.

the spectra corresponding to fully dehydroxylated samples (Figs. 4 and 5), together with the simultaneous perturbation observed on the O–H stretching band (Figs. 2 and 3), enables the unequivocal assignment of the 2165 cm^{-1} band to the C–O stretching mode of hydrogen-bonded carbon monoxide.

More specifically, in the O–H stretching region (see Fig. 2) dosing with CO brings about considerable erosion of the 3650 cm^{-1} band with attendant formation of a new IR absorption band centered at 3510 cm^{-1}. We note that, in agreement with the experimental results, a pronounced increase of both intensity and band width are expected upon hydrogen bonding (37). The observed downward shift, which amounts to 140 cm^{-1}, can be used as a comparative measurement of Brønsted acidity of OH groups in partially hydroxylated sulfated zirconia. For comparison, corresponding data for other materials are reported in Table 2. It is apparent that sulfated zirconia (not severely heat-treated) has a family of surface hydroxyls with Brønsted acidity intermediate between that of γ-alumina and that of many zeolites. When compared with pure zirconia, it is also clear that presence of sulfates enhances Brønsted acidity.

3.3. FTIR Spectra of Adsorbed Pyridine

Figure 6 shows room temperature IR spectra, in the 1675–1425-cm^{-1} region, of pyridine adsorbed on the different sulfated-zirconia samples. These spectra were taken after equilibrating the samples (at room temperature) with pyridine vapor followed by degassing at 423 K for 5 min in order to drive off physisorbed species. The general features of the spectra are similar to those reported in the literature (15–17) for other sulfated zirconias.

Interactions of pyridine, via the nitrogen lone-pair electrons with aprotic (Lewis) and protonic (Brønsted) acid sites, can be sensitively detected by monitoring the ring vibration modes 8a and 19b, named according to the nomenclature introduced by Wilson (43). These modes, which

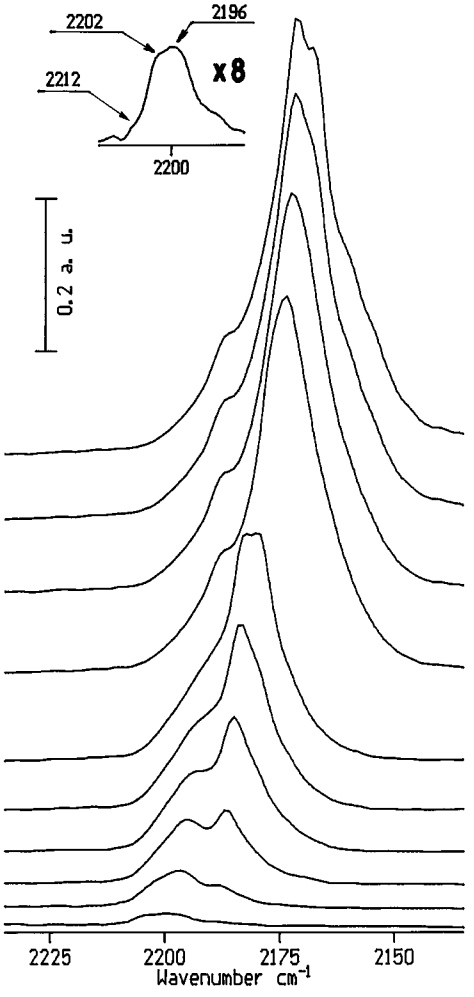

FIG. 5. Low-temperature IR spectra of CO adsorbed on SZ1173 at increasing equilibrium pressure (from *ca.* 10^{-2} to 20 Torr). Inset shows an enlarged section of the bottom spectrum in the main figure.

TABLE 1

IR Absorption Maxima for CO Adsorbed on Different Zirconia Samples. Data Correspond to Measurements Carried out at Room Temperature, Except for Those of the Present Work

Sample	ν_{CO} (cm^{-1})	References
Pure zirconia	2201 2197 2190	(10, 29, 30)
Sulfated zirconia, prepared by impregnation	2208 2202 2197	(21)
Sulfated zirconia, prepared by gas-phase doping	2212 2202	(10)
Sulfated zirconia, ex-$Zr(SO_4)_2 \cdot 4H_2O$	2212 2202 2196 2188	Present work

appear at 1580 (8a) and 1439 (19b) cm^{-1} for gas-phase pyridine (44), undergo upward shifts upon coordination of the molecule with either type of acid site. Specifically, wavenumber values in the 1635–1600 cm^{-1} range are characteristic for the 8a mode of Lewis type adducts, while smaller upward shifts are expected for the 19b mode. They are observed at 1580 to 1638 cm^{-1} (8a) and at 1440 to 1545 cm^{-1} (19b) after interaction with Brønsted acid sites, the highest wavenumbers (in each group) corresponding to the combined C–C stretching and N–H bending modes of protonated pyridine (45, 46).

Samples SZ673 and SZ873 (Figure 6) show strong IR absorption bands at 1610 and 1444 cm^{-1}, which are assigned (respectively) to the 8a and 19b modes of adsorbed pyridine forming Lewis-type adducts with coordinatively unsaturated Zr^{4+} ions. Close inspection shows that these bands shift slightly towards lower wavenumbers upon increasing the temperature of the heat treatment, corresponding values for sample SZ1173 being 1605 and 1441 cm^{-1}, respectively. This correlates with the results obtained by using

TABLE 2

Downward Shift ($\Delta\nu_{OH}$) upon Interaction of Surface Hydroxyls with Adsorbed CO at Low Temperature

Material	$\Delta\nu_{OH}$ (cm^{-1})	References
SiO_2	78	(38)
γ-Al_2O_3	95	(39)
Mordenite	294	(40)
Zeolite H–Y	273	(41)
H–ZSM-5	308	(41)
Pure zirconia	90	(42)
Sulfated zirconia	140	Present work

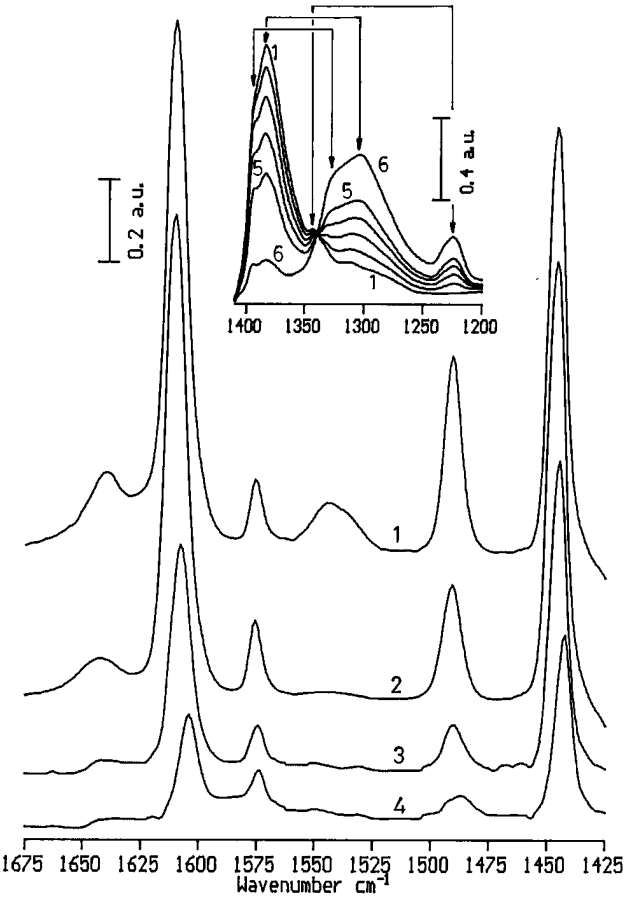

FIG. 6. Room temperature IR spectra of pyridine adsorbed on the different zirconia samples: **1**, SZ673; **2**, SZ873; **3**, SZ1073; **4**, SZ1173. Inset shows the sulfate region for sample SZ1073 (spectrum **1**), and the effect of increasing amounts of adsorbed pyridine (spectra **2**–**6**).

CO as the spectroscopic probe, since pyridine is unable to discriminate between Lewis sites of comparable strength, and weaker sites are created when temperature is increased (Section 3.2). The 8b and 19a modes of adsorbed pyridine (observed at 1574 and 1490 cm^{-1}, respectively, in the spectra of Fig. 6) will not be discussed, since they are less sensitive to the nature of pyridine-adsorbent interactions.

Regarding Brønsted acidity, the IR spectra of samples SZ673 and SZ873 show broad absorption bands around 1640 and 1544 cm^{-1} which are readily assigned to pyridine interacting with Brønsted acid sites: modes 8a and 19b, respectively. Close agreement of the corresponding wavenumbers with the values expected for the pyridinium ion (see above) demonstrates that pyridine protonation has taken place. As expected, the spectra of samples SZ1073 and SZ1173 do not show the corresponding features, due to complete dehydroxylation during thermal treatment (compare insets in Figs. 2 to 4).

The inset in Fig. 6 shows, for sample SZ1073, the effect of adsorbed pyridine on the complex sulfate band in the

1400–1340-cm^{-1} region. Similar effects were observed for the other samples. It is clearly seen that pyridine–sulfate interaction brings about discrete shifts (and broadening) of all the components of the sulfate band, giving rise to the neat isosbestic point observed at 1338 cm^{-1}. These downward shifts are more pronounced for the components at lower frequencies, which should therefore correspond to more isolated sulfate groups for which interaction with pyridine molecules adsorbed on adjacent surface sites can be maximized. The main implication of these experimental results is that sulfate groups in our samples are (mainly) at the metal oxide surface, which had to be demonstrated for materials prepared by thermolysis of zirconium sulfate. Although less pronounced, corresponding downward shifts of the S=O infrared absorption band were also observed in the CO adsorption experiments.

3.4. Further Considerations on Brønsted Acidity

The nature of the strong Brønsted acid sites in sulfated zirconia is a debated question. While some authors (17) correlate strong Brønsted acidity with the presence of disulfates, other reports (18, 47) involve only monosulfate species. In addition, quantum chemical calculations performed by Babou *et al.* (48) suggest a role of residual water in determining Brønsted acidity. It should be acknowledged that these are difficult questions to settle from an experimental approach, since the specific behavior of a particular material could depend quite critically on preparation conditions and ulterior heat treatments. However, in an attempt to establish the factors which determine the presence of the 3650 cm^{-1} OH band in the sulfated zirconia samples reported here, we have performed the following experiment. An SZ sample was heated in a dynamic vacuum at 1073 K for 90 min to accomplish total elimination of disulfate species. The sample was then allowed to rehydrate by dosing water vapor at room temperature, followed by outgassing at 623 K to remove excess water. The IR spectrum of the sample thus prepared is shown in Fig. 7. Two high frequency O–H stretching bands are observed (Fig. 7A) at 3770 and 3668 cm^{-1}, i.e., at the same wavenumber values reported by Kustov *et al.* (18) for a sample of pure zirconia, but the 3650 cm^{-1} O–H stretching band (cf. Fig. 2) is no longer present. Strong monosulfate bands are clearly observed in Fig. 7B, but not so for the 1398 cm^{-1} component corresponding to the disulfate species (see Section 3.1). An additional feature is that the spectrum in Fig. 7B shows no evidence for adsorbed molecular water (bending mode expected at about 1600 cm^{-1}). By contrast, samples SZ673 and SZ873 did show a trace of molecular water, as shown in the inset of Fig. 7B, and they also contained disulfates, as stated in Section 3.1. We are thus led to conclude that the strong Brønsted acid sites (3650 cm^{-1} OH band) present in our SZ673 and SZ873 samples are linked to the simultaneous presence of disulfate species and of trace amounts of molecular water. It could also be argued that only one of these two species is really needed, but this cannot be discerned at the present stage.

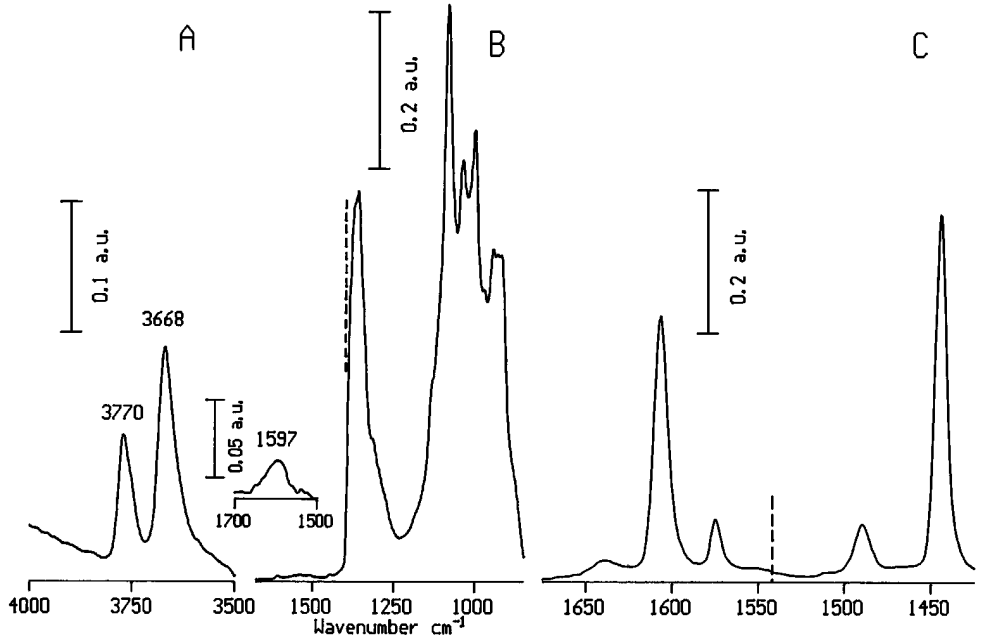

FIG. 7. IR spectra of an SZ sample heated at 1073 K (to eliminate disulfates) and then partially hydroxylated. (A) OH stretching region showing absence of the 3650-cm^{-1} band. (B) Sulfate region showing absence of disulfate species and molecular water; inset shows residual water (bending mode at 1597 cm^{-1}) for sample SZ673. (C) Spectrum of adsorbed pyridine. The dashed vertical lines mark the corresponding wavenumber values for disulfate species (B) and for the pyridinium ion (C).

Finally, Fig. 7C gives the IR spectrum of pyridine adsorbed on the zirconia sample described in this section. This spectrum is very similar to those reported by different authors (15, 49) for pyridine adsorbed on pure zirconia. The most relevant fact is the absence of the pyridinium ion band at 1544 cm^{-1} (cf. Fig. 6) This proves that the OH groups giving rise to the 3650 cm^{-1} band are directly involved in pyridine protonation on samples SZ673 and SZ873.

4. CONCLUSIONS

Thermolysis of zirconium sulfate was shown to be a method for preparing sulfated zirconia which retains a high surface area (90 $m^2 g^{-1}$) even after calcination at 1000 K, which is not usually the case with materials prepared from thermal dehydration of zirconia gels. This is a relevant feature for potential applications of the material in catalytic processes. A further advantage of the present method is that impregnation procedures, or sulfate doping from a gas phase, are not needed.

Infrared studies, using CO and pyridine as molecular probes, have shown that the sulfated zirconia samples described here are similar to those prepared by conventional routes. Sulfate species remaining after thermolysis of the zirconium sulfate precursor were found to be mainly at the metal oxide surface, which showed enhanced Brønsted and Lewis acidity, as compared with pure (partially hydroxylated) zirconia.

Several families of Lewis acid sites were revealed by low temperature adsorption of CO: there are IR absorption bands at 2212, 2202, 2196, and 2188 cm^{-1}. Pyridine gave corresponding Lewis-type adducts which adsorbed at 1610 and 1444 cm^{-1}.

In the OH stretching region two main bands were found at 3750 and at 3650 cm^{-1}. The OH groups giving rise to the 3650 cm^{-1} band showed strong Brønsted acidity. This was demonstrated by (i) the ability of these hydroxyl groups to protonate pyridine, and (ii) the observed frequency shift down to 3510 cm^{-1} upon interaction with CO at 77 K. This frequency shift, $\Delta\nu_{OH} = 140\ cm^{-1}$, was measured here for the first time on sulfated zirconias, and it suggests that Brønsted acidity of these materials is intermediate between that of partially hydroxylated γ-alumina (corresponding $\Delta\nu_{OH} = 95\ cm^{-1}$) and that shown by protonic forms of zeolites, with $\Delta\nu_{OH}$ values in the 270–310 cm^{-1} range. For comparison, the corresponding value for pure zirconia is $\Delta\nu_{OH} = 90\ cm^{-1}$.

Detailed studies reported here have shown that sulfated zirconia samples having enhanced Brønsted acidity also show the presence of disulfate species and traces of residual water. When both of these species are eliminated Brønsted acidity declines. However, it has not been possible to discern whether both, viz., molecular water and disulfate species, are needed for enhanced Brønsted acidity or whether only one of them is sufficient.

ACKNOWLEDGMENTS

This work has been supported by the Spanish DGICYT, Ref. PB93-0425. The Ministerio de Educación y Ciencia is gratefully acknowledged for support of the sabbatical stay of A. Zecchina at the Universidad de las Islas Baleares.

REFERENCES

1. Jin, T., Yamaguchi, T., and Tanabe, K., *J. Phys. Chem.* **90**, 4794 (1986).
2. Arata, K., *Adv. Catal.* **37**, 165 (1990).
3. Parera, J. M., *Catal. Today* **15**, 481 (1992).
4. Chen, F. R., Coudurier, G., Joly, J. F., and Vedrine, J. C., *J. Catal.* **143**, 616 (1993).
5. Iglesia, E., Soled, S. L., and Kramer, G. M., *J. Catal.* **144**, 238 (1993).
6. Morterra, C., Cerrato, G., Pinna, F., Signoretto, M., and Strukul, G., *J. Catal.* **149**, 181 (1994).
7. Adeeva, V., de Haan, J. W., Jänchen, J., Lei, G. D., Schünemann, V., van de Ven, L. J. M., Sachtler, W. M. H., and van Santen, R. A., *J. Catal.* **151**, 364 (1995).
8. Hsu, C. Y., Heimbruch, C. R., Armes, C. T., and Gates, B. C., *J. Chem. Soc. Chem. Comm.* **1645**, (1994).
9. Kazansky, V. B., *Acc. Chem. Res.* **24**, 379 (1991).
10. Bensitel, M., Saur, O., Lavalley, J. C., and Mabilon, G., *Mater. Chem. Phys.* **17**, 249 (1987).
11. Escalona Platero, E., and Peñarroya Mentruit, M., *Catal. Lett.* **30**, 31 (1995).
12. Escalona Platero, E., and Peñarroya Mentruit, M., *Mater. Lett.* **14**, 318 (1992).
13. Otero Areán, C., and Escalona Platero, E., *Adsorption Sci. Technol.* **1**, 159 (1984).
14. Komarov, V. S., and Sinilo, M. F., *Kinet. Katal.* **29**, 605 (1988).
15. Waqif, M., Bachelier, J., Saur, O., and Lavalley, J. C., *J. Mol. Catal.* **72**, 127 (1992).
16. Morterra, C., Cerrato, G., and Bolis, V., *Catal. Today* **17**, 505 (1993).
17. Morterra, C., Cerrato, G., Emanuel, C., and Bolis, V., *J. Catal.* **142**, 349 (1993).
18. Kustov, L. M., Kazansky, V. B., Figueras, F., and Tichit, D., *J. Catal.* **150**, 143 (1994).
19. Bensitel, M., Saur, O., Lavalley, J. C., and Morrow, B. A., *Mater. Chem. Phys.* **19**, 147 (1988).
20. Morterra, C., Cerrato, G., Pinna, F., and Signoretto, M., *J. Phys. Chem.* **98**, 12373 (1994).
21. Morterra, C., Bolis, V., Cerrato, G., and Magnacca, G., *Surf. Sci.* **307/309**, 1206 (1994).
22. Babou, F., Coudurier, G., and Védrine, J. C., *J. Catal.* **152**, 341 (1995).
23. Nakano, Y., Iizuka, T., Hattori, H., and Tanabe, K., *J. Catal.* **57**, 1 (1978).
24. Otero Areán, C., Fernández Colinas, J. M., Mata Arjona, A., and Villa García, M. A., *An. Quim.* **78**, 146 (1982).
25. Villa García, M. A., Trobajo Fernández, M. C., and Otero Areán, C., *Thermochim. Acta* **126**, 33 (1988).
26. Marchese, L., Bordiga, S., Coluccia, S., Martra, G., and Zecchina, A., *J. Chem. Soc. Faraday Trans.* **89**, 3483 (1993).
27. Yamaguchi, T., Jin, T., and Tanabe, K., *J. Phys. Chem.* **90**, 3148 (1986).
28. Morterra, C., Orio, L., and Emanuel, C., *J. Chem. Soc. Faraday Trans.* **86**, 3003 (1990).
29. Morterra, C., Orio, L., Bolis, V., and Ugliengo, P., *Mater. Chem. Phys.* **29**, 457 (1991).
30. Morterra, C., Bolis, V., Fubini, B., Orio, L., and Williams, T. B., *Surf. Sci.* **251/252**, 540 (1991).
31. Hammaker, R. M., Francis, S. A., and Eischens, R. P., *Spectrochim. Acta* **21**, 1295 (1965).
32. Persson, B. N. J., and Ryberg, R., *Phys. Rev. B* **24**, 6954 (1981).

33. Escalona Platero, E., Scarano, D., Spoto, G., and Zecchina, A., *Faraday Discuss. Chem. Soc.* **80**, 183 (1985).
34. Zecchina, A., Scarano, D., and Garrone, E., *Surf. Sci.* **165**, 492 (1985).
35. Scarano, D., and Zecchina, A., *J. Chem. Soc. Faraday Trans. 1* **82**, 3611 (1986).
36. Zecchina, A., Escalona Platero, E., and Otero Areán, C., *J. Catal.* **107**, 244 (1987).
37. Pimentel, G. C., and McClellan, A. L., "The Hydrogen Bond." Freeman, San Francisco, 1960.
38. Ghiotti, G., Garrone, E., Morterra, C., and Boccuzzi, F., *J. Phys. Chem.* **83**, 2863 (1979).
39. Knözinger, H., *in* "Elementary Reaction Steps in Heterogeneous Catalysis" (R. W. Joyner and R. A. van Santen, Eds.), p. 267. Kluwer, Amsterdam, 1993.
40. Bordiga, S., Lamberti, C., Geobaldo, F., Zecchina, A., Turnes Palomino, G., and Otero Areán, C., *Langmuir* **11**, 527 (1995).
41. Makarova, M. A., Al-Ghefaili, K. M., and Dwyer, J., *J. Chem. Soc. Faraday Trans.* **90**, 383 (1994).
42. Escalona Platero, E., and Peñarroya Mentruit, M., unpublished.
43. Wilson, E. B., *Phys. Rev.* **45**, 706 (1934).
44. Basila, M. R., Kantner, T. R., and Rhee, K. H., *J. Phys. Chem.* **68**, 3197 (1964).
45. Parry, E. P., *J. Catal.* **2**, 374 (1963).
46. Zerbi, G., Crawford, B., and Overend, J., *J. Chem. Phys.* **38**, 127 (1963).
47. Riemer, T., Spielbauer, D., Hunger, M., Mekhemer, G. A. H., and Knözinger, H., *J. Chem. Soc., Chem. Comm.* 1181 (1994).
48. Babou, F., Bigot, B., and Sautet, P., *J. Phys. Chem.* **97**, 11501 (1993).
49. Morterra, C., and Cerrato, G., *Langmuir* **6**, 1810 (1990).